

experimental value of 39.9 kN/m, which corresponds to a safe-side difference of 12 percent.

The live-load effects in a soil-steel structure may not be very sensitive to the soil properties (5,6), but they certainly should be to the flexural stiffness of the relieving slab. Clearly, a structure with a very thin relieving slab will tend to behave more like a structure without a relieving slab than like the McIntyre River structure.

The simple method of analysis just given does not take into account the relative stiffness of the relieving slab as opposed to that of the whole structure. This method should therefore be used as an interim measure for structures similar to the tested one until an analytical method is developed that can rationally take account of the load dispersion in both the longitudinal and transverse directions of the conduit.

#### CONCLUSIONS

The comparison of test results on a soil-steel structure with a relieving slab with those on an identical but smaller structure without the slab shows that the relieving slab has the effect of considerably reducing the live-load thrusts in the conduit wall. For the structure tested, the maximum thrusts were reduced by about 50 percent. Live-load moments were negligibly small.

The relieving slab of the tested structure appeared to disperse concentrated loads at a slope of 1 vertical to 1.75 horizontal in all directions.

#### REFERENCES

1. B. Bakht. Soil-Steel Structure Response to Live Loads. Journal of the Geotechnical Division, ASCE, June 1981, pp. 779-798.
2. C. Fung. Elliptical K-D Steel Pipe for the City of Thunder Bay, Ontario: Design, Instrumentation and Field Testing. Westeel Roscoe Limited, Toronto, Ontario, Canada, 1974.
3. B. Bakht and P.F. Csapoly. Bridge Testing. Structural Research Report. Research and Development Branch, Ministry of Transportation and Communications, Downsview, Ontario, Canada, 1979.
4. B. Bakht and Z. Knobel. Testing of a Soil-Steel Structure with a Relieving Slab. Structural Research Report SRR-84-4. Research and Development Branch, Ministry of Transportation and Communications, Downsview, Ontario, Canada, Jan. 1984.
5. G. Abdel-Sayed and B. Bakht. Analysis of Live-Load Effects in Soil-Steel Structures. In Transportation Research Record 878, TRB, National Research Council, Washington, D.C., 1982, pp. 49-55.
6. M.G. Katona, J.M. Smith, R.S. Odells, and J.R. Allgood. CANDE--A Modern Approach for the Structural Design and Analysis of Buried Culverts. Report FHWA-RD-77-5. FHWA, U.S. Department of Transportation, Oct. 1976.

Publication of this paper sponsored by Committee on Subsurface Soil-Structure Interaction.

## Inelastic Buckling of Soil-Steel Structures

MEDHAT GHOBRIAL and GEORGE ABDEL-SAYED

#### ABSTRACT

The buckling of composite soil-steel structures is examined, taking into consideration the formation of plastic hinges in the conduit walls. A structural model is applied in which the soil is replaced by discrete normal and tangential springs acting at the nodal points of a closed polygon of beam elements representing the conduit. The coefficient of the soil springs is taken to be dependent on the type of soil as well as on the direction of displacement and depth of soil at the surface of contact with the conduit. A nonlinear matrix analysis is applied to examine the stability problems in the conduit. Numerical examples show two distinctive modes of failure. A snap-through failure is observed in conduits with relatively large spans or shallow cover or both, whereas short-span conduits with deep cover exhibit no sudden buckling but instead displacements with a higher rate of increase after each loading step. The analyses show reasonable agreement with the results of the failure load obtained from the Ontario Highway Bridge Design Code for the case of cylindrical conduits. However, it is found that the code overestimates the failure load for the horizontal ellipse, whereas it underestimates that for the vertical ellipse.

Underground flexible conduits are being constructed more widely and have proven to be practical and economical alternatives to short-span bridges. Their high load-carrying capacity is due to the interaction between their wall displacement and the pressure induced in the surrounding engineered soil.

According to the current design codes (1,2), the design of the flexible conduits is governed mainly by the circumferential thrust induced in the conduit walls. If the depth of cover is equal to or more than a minimum specified depth of one-sixth of the span, moments in the wall are not required to be calculated. The justification for the neglect of moment lies in the manner in which the interface pressure between the steel conduit wall and the surrounding soil mass changes with the movement of the wall. Even if a bending moment occurs locally to cause partial yielding, the resulting movement of the wall causes an increase in the interface pressure provided by the adjacent soil mass, and this increase in pressure tends to inhibit any further movement.

Therefore, the load-carrying capacity of the culvert is governed mainly by the compression failure, which could occur in one of two basically different forms. One is a wall-crushing (crippling) failure that occurs when the stresses approach the yield point of the material. This type of failure was observed in conduits with low wall flexibility buried in soil of high passive earth resistance (3). The second type is a snap-through buckling in which a localized reversal of curvature occurs in the ring. Such failure can occur in conduits of high ring flexibility embedded in soil with low passive resistance.

Earlier investigators gave little attention to buckling as a criterion for corrugated metal conduits. As long as a sufficiently high standard of fill placement was provided in the vicinity of the culvert, either deformation (4,5) or ring stress (6) criteria were considered sufficient to ensure the safety of the structure. Field performance in general has confirmed the validity of this approach for the common field conditions and small conduits.

In recent years a general increase in conduit size and loadings has required more refinements of the old design methods. This has led to considerable progress in research for the prebuckling behavior of the conduit (7-9).

The stability of soil-steel structures has also been examined (8,10-12). However, almost all current stability studies are based on uniformly applied pressure on circular conduits. Also, the coefficient of soil reaction is assumed to be constant over the conduit wall irrespective of its direction or the depth of soil at its point of action. The Ontario Highway Bridge Design Code (OHBDC) and the AASHTO specifications are based on these studies. Their formulas are extended, without proof, to noncircular cross sections by treating the conduit as a circular one with a radius equal to that of the radius of curvature at the crown. Recently, Okeagu (13) applied an energy approach to examine the stability of conduits of different configurations. He also considered the variation of the coefficient of soil reaction around the conduit but limited his work to the elastic behavior of the conduit walls.

The objective of this paper is to examine the buckling of large-span flexible conduits with different configurations. Consideration is given to the effect of nonuniform pressure due to live loads as well as to the variation of the coefficient of soil reaction around the conduit. The formation of plastic hinges in the conduit walls is also accounted for.

#### COEFFICIENT OF SOIL REACTION

Recent studies by Okeagu and Abdel-Sayed (14) found the normal coefficients of soil reaction ( $k_n$ ) to vary around the conduit, which may be expressed as follows:

$$k_n = \gamma \beta C_d C_\theta (H/D)^{1/2} \quad (1)$$

in which

$$C_d = 4.25 - (0.75D/100) \quad (1a)$$

$$C_\theta = 0.25 [1 + 5.4 (\theta/\pi)] \quad (1b)$$

$\beta = 1.0$  for dense compacted granular fill

$$= 0.45 + (D/200) [(\theta/\pi) - 0.5]^2 \text{ for medium dense compacted fill} \quad (1c)$$

where

$H$  = depth of fill at point where  $k_n$  is computed (in.),

$D$  = span of conduit (in.),

$\gamma$  = unit weight of soil (lb/in.<sup>3</sup>),

$\theta$  = angular coordinate in radians

(see Figure 1), and

$\beta$ ,  $C_d$ , and  $C_\theta$  = factors involved in calculating coefficient of soil reaction.

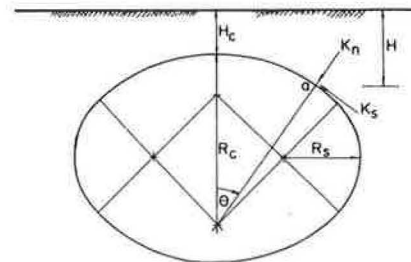


FIGURE 1 Geometry of a practical ellipse and angular coordinates.

Figure 2 shows the variation of the coefficient  $k_n$  for the case of a circular conduit with  $D = 300$  in. and depth of cover  $H_c = 48$  in.

The tangential coefficient of soil reaction ( $k_s$ ) is found to be constant and about 20 percent of the coefficient  $k_n$  at the invert of the conduit.

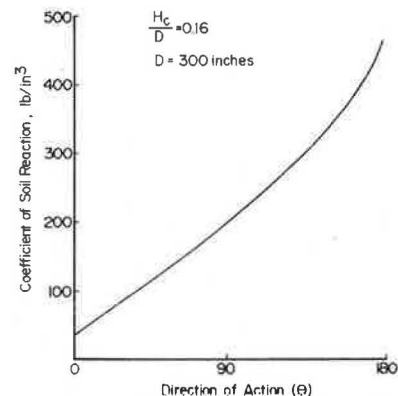


FIGURE 2 Variation of coefficient of soil reaction.

STABILITY ANALYSIS

The stability analysis is based on considering a plane slice of unit width of the conduit and the surrounding soil. This approach is generally accepted for the analysis and stability problems in soil-steel structures because the loading conditions are assumed not to vary in the lateral direction.

The structural model chosen to simulate the soil-conduit structure interaction is shown in Figure 3. The soil medium is replaced by a group of pairs of linear radial and tangential springs acting at the nodal points of the closed polygon of beam elements representing the conduit. The spring coefficients are calculated by using the coefficients of soil reaction ( $k_n$  and  $k_g$ ) as outlined previously. These coefficients are dependent on the type and depth of soil as well as on the direction of displacement of the conduit wall.

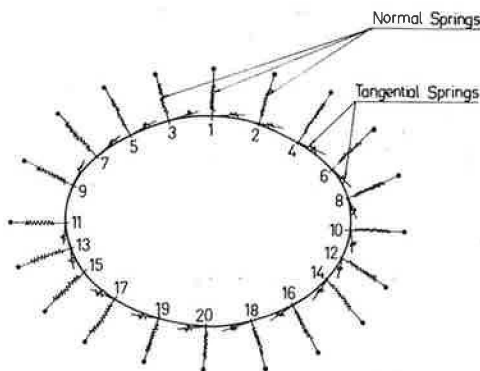


FIGURE 3 Structural model of the soil-conduit interaction.

Within the range of small displacements, Okeagu (13) found the coefficients of soil reaction to be independent of the magnitude of displacement. This observation is considered to be valid in this study, in spite of the relatively large displacement at failure. This is based on the assumption that no shear or plastic failure takes place within the soil media. Thus, the current analysis is concerned with the stability problem in the conduit walls under stable soil response, which is replaced by elastic supports.

The second-order elastic-plastic analysis of the planar frame on elastic supports is conducted by using a piecewise elastic regime in the elastic-plastic deformation of a member. The effect of the axial force is taken into account by means of a stability function, and a delta function is used to define the formation as well as the unloading of plastic hinges.

FORMULATION OF PLASTIC HINGES

The beam elements of the conduit wall are allowed to exhibit plastic deformation at one or both ends of each element when the bending moment acting at the node reaches a critical plastic moment value ( $M_p$ ) according to the following formula (8):

$$M_p = M_T (1 - n^2) \tag{2}$$

where

$$M_T = f_y \cdot Z, \\ Z = \text{plastic section modulus (in.}^3\text{),}$$

$$n = F/F_T, \\ F_T = f_y \cdot A \text{ (lb),} \\ F = \text{axial force acting through the section (lb),} \\ A = \text{cross-sectional area of conduit wall per unit width (in.}^2\text{/in.), and} \\ f_y = \text{yield point of the conduit material (lb/in.}^2\text{).}$$

STIFFNESS MATRIX

The element stiffness matrix is generated to describe the element in its pure elastic stage before formation of plastic hinges and after the formation of hinges.

Before formation of plastic hinges, the stiffness equation describing the behavior of an element  $ij$  can be written as follows:

$$\{F\} = [K] \{W\} + P[S] \{W\} \\ = [K + PS] \{W\} \tag{3}$$

where

- {F} = external load vector (6 x 1),
- {W} = load vector of the element (6 x 1),
- [K] = elastic stiffness matrix containing linear terms (6 x 6),
- [S] = geometric stiffness matrix of the element (6 x 6), and
- P = axial internal force component acting through the element (negative if in compression).

The formation of plastic hinges at one or both ends of a beam element  $ij$  can be accounted for through the following general equation (15):

$$\begin{Bmatrix} F \\ 0 \end{Bmatrix}_{\substack{6 \times 1 \\ 2 \times 1}} = \begin{bmatrix} K_{11} & K_{12} \\ K_{21} & K_{22} \end{bmatrix} \begin{Bmatrix} W \\ \theta \end{Bmatrix}_{\substack{6 \times 1 \\ 2 \times 1}} + P \begin{bmatrix} S_{11} & S_{12} \\ S_{21} & S_{22} \end{bmatrix} \begin{Bmatrix} W \\ \theta \end{Bmatrix}_{\substack{6 \times 1 \\ 2 \times 1}} + \begin{Bmatrix} 0 \\ Q \end{Bmatrix}_{\substack{6 \times 1 \\ 2 \times 1}} \tag{4}$$

where

- $[K_{11}], [K_{12}], [K_{21}],$  and  $[K_{22}]$  = stiffness submatrices in general stiffness equation containing linear terms,
- $[S_{11}], [S_{12}], [S_{21}],$  and  $[S_{22}]$  = geometric submatrices in general stiffness equation of element,
- {Q} = vector describing additional nodal load due to formation of plastic hinge, and
- {θ} = vector describing the end slope beyond and inside plastic hinge section.



$$\{\theta\}_{2 \times 1} = \begin{Bmatrix} \theta_{ij} \\ \theta_{ji} \end{Bmatrix}$$

$$\begin{aligned} \Delta_{ij} &= 0 \text{ if } M_{ij} < M_p, \\ \Delta_{ij} &= 1 \text{ if } M_{ij} = M_p, \\ \Delta_{ji} &= 0 \text{ if } M_{ji} < M_p, \text{ and} \\ \Delta_{ji} &= 1 \text{ if } M_{ji} = M_p. \end{aligned}$$

Equation 4 can be divided into the two following equations:

$$\{F\} = [K_{11} + PS_{11}] \{W\} + [K_{12} + PS_{12}] \{\theta\} \quad (5a)$$

and

$$\{\theta\} = [K_{21} + PS_{21}] \{W\} + [K_{22} + PS_{22}] \{\theta\} + \{Q\} \quad (5b)$$

Equation 5b can be written as the following:

$$\{\theta\} = -[K_{22} + PS_{22}]^{-1} ([K_{21} + PS_{21}] \{W\} + \{Q\}) \quad (6)$$

Substituting Equation 6 into Equation 5a to eliminate the vector  $\{\theta\}$  results in the following equation:

$$\{F\} = ([K_{11} + PS_{11}] - [K_{12} + PS_{12}] [K_{22} + PS_{22}]^{-1} [K_{21} + PS_{21}]) \{W\} - ([K_{12} + PS_{12}] [K_{22} + PS_{22}]^{-1}) \{Q\} \quad (7)$$

Equation 7 is the general stiffness equation for an element having zero, one, or two plastic hinges acting at the element's ends as shown in Table 1.

Equation 7 can be simplified as follows:

$$\{\bar{F}\}_p = [\bar{K}]_p \{W\} \quad (8)$$

where  $\{\bar{F}\}_p$  is the general load vector =  $\{F\} + [K_{12} + PS_{12}] [K_{22} + PS_{22}]^{-1} \{Q\}$  and  $[\bar{K}]_p$  is the general elastic-geometric stiffness matrix =  $[K_{11} + PS_{11}] - [K_{12} + PS_{12}] [K_{22} + PS_{22}]^{-1} [K_{21} + PS_{21}]$ . The size of  $\bar{K}_p$  can be 6 x 6, 5 x 5, or 4 x 4 for elements having zero, one, or two plastic hinges, respectively.

TABLE 1 Edge Conditions of Beam Elements

Case	Substitution	Description
1	$\Delta_{ij} = \Delta_{ji} = 0.0$	Elastic behavior
2	$\Delta_{ij} = 1.0, \Delta_{ji} = 0.0$	Plastic hinge at end i
3	$\Delta_{ij} = 0.0, \Delta_{ji} = 1.0$	Plastic hinge at end j
4	$\Delta_{ij} = \Delta_{ji} = 1.0$	Plastic hinges at both ends

A computer program has been written to perform the foregoing analysis. The effect of the dead load is accounted for as initial thrust ( $T_D$ ) calculated by using the formula of the OHBDC (1):

$$T_D = \mu_1 \sigma_{vo} R_c \quad (9)$$

where

$\sigma_{vo}$  = the free field overburden pressure,  
 $R_c$  = radius of curvature at crown, and  
 $\mu_1$  = conduit shape factor (Figure 4).

The live load is applied at the embankment level in the form of two rear axle loads with spacing  $x = 62$  in. (Figure 5). The load is considered to be dispersed at a slope 1:1 in the span direction and 2

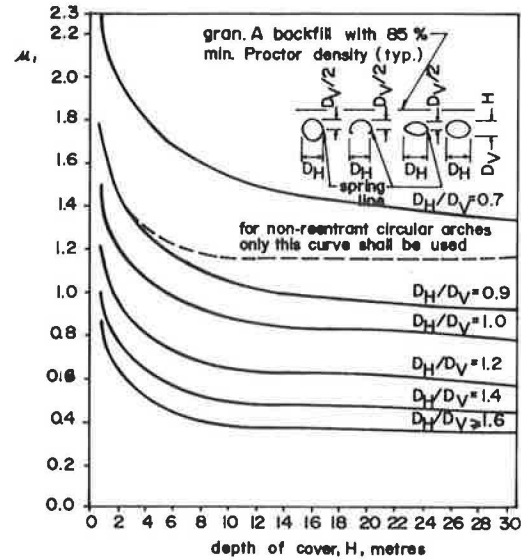


FIGURE 4 Conduit shape factor versus depth of cover.

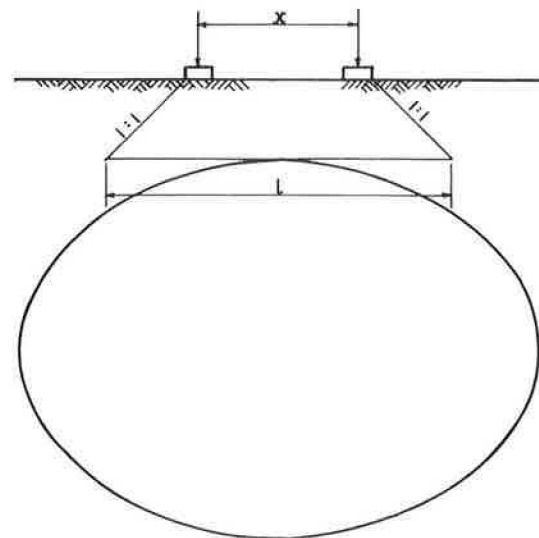


FIGURE 5 Live-load dispersion in span direction.

vertical to 1 horizontal in the lateral direction [OHBDC (1)]. The soil pressure, induced by the live load, is calculated at the crown level and is considered to be acting normal to the conduit within the range of its action ( $l$ ).

The live load is applied incrementally and the displacement and internal force components are computed after each step. When a normal spring is subjected to tension, the coefficients of both radial and tangential springs acting at that node are reduced to zero in the next loading step and up to failure. This stimulates a separation between the outside surface of the conduit and the surrounding soil.

The analysis has been conducted for conduits with different span/height ratios and under different depths of cover ( $H_c$ ).

The results obtained from the analysis are shown in Table 2. Also, Figure 6 shows the general trend of failure load versus the span/height ratio with different depths of soil cover. [In Figure 6,  $N$  is the ratio of axle load at failure to the axle load of the testing truck ( $P_a$ ) in pounds per pound and

TABLE 2 Development of Plastic Hinges and Ultimate Load-Carrying Capacity

Conduit Dimension			Hinge Formation						Failure Load		Axial Stress at Failure			
			First		Second		Third				P (kips)	N	OHBDC (ksi)	Analysis (ksi)
A (in.)	B (in.)	H <sub>c</sub> (in.)	Joint No.	N	Joint No.	N	Joint No.	N						
300	300	36	1	5.28	4,5	7.26	2,3	8.38	390	8.38	11.61	14.87	0.79	6.4
		48	1	7.26	4,5	9.9	2,3	11.2	510	9.9	15.11	15.17	1.00	6.8
		60	1,4,5	5.28	6,7	5.94		12.5	570	12.5	18.36	22.85	0.80	6.8
		72	1	7.0	2,3	10.0	4,5	14.0	637	14.0	20.87	30.18	0.69	7.3
		84	1	7.0	2,3	10.0		15.0	652	15.0	22.65	28.02	0.81	12.4
200	200	36	1	6.6	2,3	12			764	16.8	17.88	17.00	1.05	5.4
		48	1	7.0	2,3	12	4,5	21	955	21.0	21.87	19.56	1.12	9.0
		60	1	10.5	2,3	16.5	4,5	31.5	1,433	31.5	24.23	22.27	1.09	13.8
		72	1	12	2,3,4,5	19.5	6,7	24	1,560	34.5	25.80	23.41	1.10	13.2
		84	1	18.5	2,3	22.5			1,842	40.5	26.91	23.82	1.13	
150	150	36	1	8	4,5	14	2,3	16	1,092	24	22.27	23.84	0.93	6.5
		48	1	12	2,3,4,5	20			1,635	36	25.17	24.57	1.02	8.87
		60	6,7	24	1	28	2,3	42	1,957	43	26.89	25.77	1.04	2.03
		72	4,5,6,7	12.5	2,3	17.5			2,047	45	28.03	35.29	0.79	2.01
300#M	250	36	1	1.66	4,5	2.66	2,3	3.0	151.5	3.33	9.43	14.13	0.66	8.07
		48	1	2.33	2,3,4,5	4.0			212.0	4.66	12.34	15.80	0.78	9.2
		60	1	2.66	2,3	4.66	4,5	5.66	269	5.98	15.07	16.80	0.89	9.97
		72	1	3.96	2,3	5.94			394	8.65	17.65	18.34	0.96	12.02
		84	1	4.66	2,3	7.32	4,5	9.9	479	10.6	19.88	19.77	1.01	13.56
300#M	200	36	1	1.33	4,5	1.66			106	2.33	7.25	10.16	0.71	5.8
		48	1	1.65	4,5	2.33			135.5	3.00	9.53	11.72	0.81	6.7
		60	1	2.5	4,5	3.0			204.7	4.50	11.70	13.30	0.87	11.1
		72	1	3.0	4,5	4.0			227.5	5.0	13.77	13.81	1.00	14.1
		84	1	3.33	4,5	4.66			273	6.0	15.73	15.44	1.01	7.08
300#M	150	36	1	1.33	4,5	1.66			91	2.0	5.09	4.55	1.09	3.40
		48	1	1.66	4,5	2.0			106	2.33	6.73	5.12	1.31	3.03
		60	1	1.66					106	2.33	8.31	7.70	1.07	4.40
		72	1	2.0	4,5	3.3			159	3.50	9.83	9.10	1.08	5.20
		84	1	2.50	6,7	3.0			159	3.50	11.29	10.93	1.03	6.42
300#M	400	36	4,5	4.32	2,3	6.0			659	14.5	8.42	19.47	0.43	3.20
		48	1	6.00	2,3	9.0			737	16.2	10.92	22.90	0.47	11.30
		60	1	9.28	2,3	7.26			1,096	24.1	13.28	16.98	0.78	16.30
		72	1	6.0	2,3	7.00			1,274	28.0	15.52	14.04	1.10	19.4
		84	1	6.5	2,3	7.50			1,510	33.2	17.66	12.98	1.36	28.4
300#M	187	36	1	1.66	4,5	2			106	2.33	6.68	6.71	1.04	7.93
		48	1,4,5	2.66					141	3.1	8.80	7.22	1.22	2.74
		60	1	3	4,5	3.3			172	3.8	10.82	10.24	1.06	5.86
		72	1	3	4,5	3.8			212	4.66	12.75	12.20	1.05	11.2
		84	1	3.33	4,5	4.0	6,7	4.66	212	4.66	14.59	13.83	1.05	4.75
300#R	187	36	1,2,3	1.66					106	2.33	6.68	7.76	0.86	3.52
		48	1	2.66	2,3	3.0			147	3.25	8.80	9.03	0.97	5.25
		60	1,2,3	3.0					186	4.1	10.82	10.75	1.01	8.7
		72	1	3.66	2,3	4			247	5.43	12.75	10.83	1.17	10.5
		84	1	4	2,3	5.1			242	6.2	14.58	10.91	1.33	12.5

Note: A = span of conduit, B = height of conduit, H<sub>c</sub> = depth of cover, N = ratio of axle load at failure to axle load of testing truck = P at failure/45.5 kips,  $\alpha$  = ratio of ultimate stress by OHBDC to the failure load by analysis,  $\Delta$  = deflection at crown at failure, #M = ellipse shape according to mathematical form, #R = ellipse composed of circular segments.

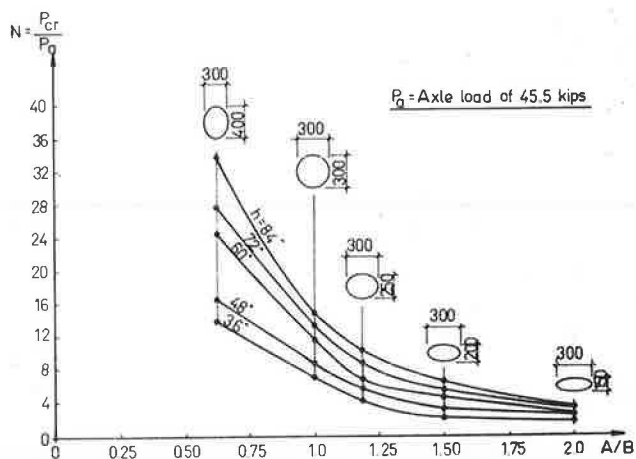


FIGURE 6 Failure load ratio versus span/height ratio with different depths of soil cover.

$P_{cr}$  is the axle load at failure in pounds. B is the height of the conduit in inches.]

OBSERVATIONS

With the exception of relatively small conduits (150-in. spans) under deep cover (60 in. and deeper), the first plastic hinge always occurs at the crown.

The second location for plastic hinges depends on the span and the depth of the soil cover. In conduits with large spans or shallow cover or both, the second location tends to be farther away from the crown (i.e., points 6 and 7) than in those with small spans or deep cover or both, where the second plastic hinge usually occurs at nodes close to the crown (i.e., 2 and 3). In most cases, however, where moderate conditions exist, the second plastic hinge usually occurs at nodes 4 and 5 (i.e., at an angle 36 degrees from the crown).

In all the cases examined, a maximum of three pairs of plastic hinges developed in addition to the hinge at the crown. Also, it was noted that all the plastic hinges developed in the upper zone of the conduit. This observation is contrary to the suggestions by Kloepfel and Glock (8) that the lower zone of the conduit may develop a number of plastic hinges and thus can be approximated by a sprocket chain on elastic supports.

Failure occurred in two distinctive modes. For conduits with relatively large spans or shallow cover or both, snap-through, sudden buckling failure was evident. In this case excessive deformation suddenly occurs at the application of the critical load, and the load-deflection diagram (Figure 7) exhibits a tendency to be asymptotic at the critical load. A second mode of failure was evident for con-

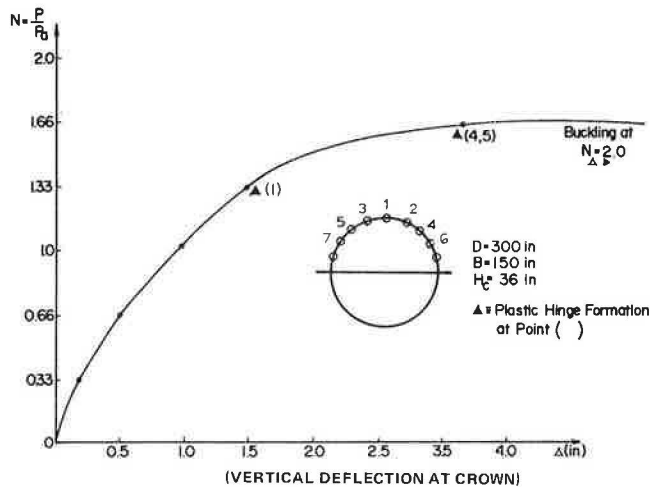


FIGURE 7 Load-deflection curve of a snap-through mode of failure.

duits with small spans or deep cover or both. In this case no real sudden buckling took place, but instead the conduit exhibited larger displacements with a higher rate of increase after each loading step until the total vertical displacement at the crown reached a value where the conduit was deemed nonfunctional and the displacement was unserviceable. The slope of the load-deflection diagram for this case decreases gradually but does not become asymptotic within the loading range as in the first case (Figure 8).

In practice, elliptical conduits are built from circular components with radii of curvature of different magnitudes at the sides and at the crown and invert. This shape is different from the mathematically formulated shape in which the curvature changes at each point along the circumference. It may be noted (Figure 9) that the assumed shape of the conduit has considerable effect on the calculated load-carrying capacity of the conduit.

In general, there is agreement in the OHBDC with the failure load obtained from the analysis for the case of circular conduits (Table 2). However, the failure load for the horizontal ellipse under deep cover tends to be overestimated whereas that of the vertical ellipse under shallow cover tends to be underestimated. This comparison is based on the assumption of medium dense compacted fill with the modification factor (8) as given in Equation 1c and a modulus of soil reaction  $E_s = 8,000$  psi in the formula of the OHBDC.

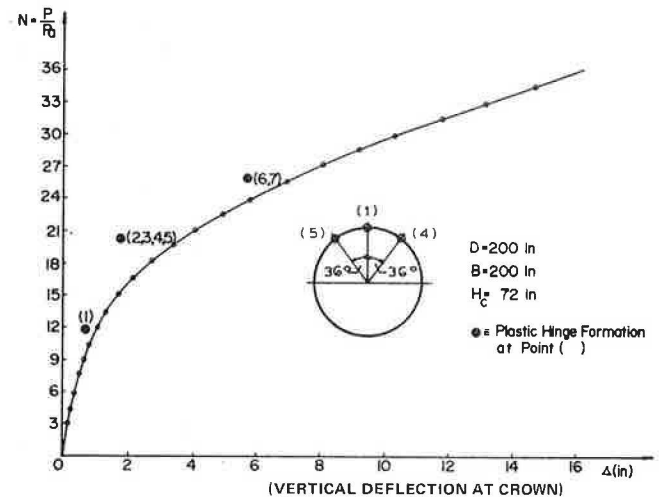


FIGURE 8 Load-deflection curve for conduits and deep cover.

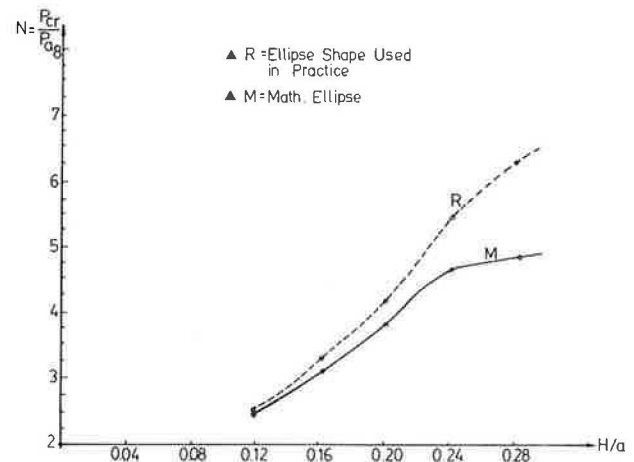


FIGURE 9 Failure load ratio versus span/height ratio for mathematically formulated elliptic shape and practical shape with circular components.

## Discussion

Tzong H. Wu\* and Nelson N. S. Chou\*\*

Inability to estimate the collapse load of buried conduits accounts for by far the largest uncertainty in the use of analytical methods to design buried conduits. The authors' work on inelastic buckling of buried pipes is certainly a step in the right direction.

Buckling of buried flexible conduits can occur at stress levels below yield or after yielding has initiated. An excellent review on buckling failure of flexible buried conduits conducted by Leonards and Stetkar (12) revealed that buckling of flexible pipes can result from three different mechanisms. An

\*Department of Civil Engineering, University of Colorado at Denver.

\*\*Colorado Department of Highways, Denver.



"elastic local buckling" involves a small percentage of the pipe circumference and occurs before any plastic deformation develops in the pipe wall. "Elastic buckling" in high buckling modes involves the entire pipe circumference and also occurs before plastic deformation occurs in the pipe wall. "Inelastic buckling" is accompanied by plastic yielding of the pipe wall and usually develops in a low buckling mode. Elastic buckling occurs at relatively small pipe deflections, whereas inelastic buckling is often associated with large deflections. In both cases, however, buckling occurs when large strains develop.

We suspect the validity of the authors' assumption that the coefficients of soil reaction (Equation 1) obtained from small displacements are applicable to conditions in which large displacements occur. The authors state that this is valid "in spite of the relatively large displacement at failure. This is based on the assumption that no shear or plastic failure takes place within the soil media. Thus, the current analysis is concerned with the stability problem in the conduit walls under stable soil response, which is replaced by elastic supports." It does not appear reasonable to us that the soil will remain elastic when the conduit (hence the soil surrounding the conduit) has undergone large displacements. Perhaps more important, it is not clear whether the analyses presented in the paper were carried out by using the small-strain or large-strain formulation. We have always held the view that the only way to analyze buckling in a rational manner is to employ the large-deformation theory. Whenever buckling takes place, it is always associated with large strains.

Finally, the authors present a comparison with the failure loads obtained from the OHBDC and conclude that the OHBDC agrees well with the analyses for circular conduits and that the code overestimates the failure load for horizontal elliptical conduits and underestimates that of vertical elliptical conduits. The analyses were carried out by assuming a constant modulus of soil reaction ( $E_s$ ) of 8,000 psi. We wonder how the value of  $E_s$  was selected. If the value of  $E_s$ , which is a parameter of a high degree of uncertainty, was varied to a certain degree, would the authors have drawn the same conclusion?

## Authors' Closure

The performance limit for buried corrugated steel pipes is not a single phenomenon, but the interaction of a number of phenomena (3). These include the stability of the conduit walls as well as the shear or plastic failure that takes place within the soil media. These failure criteria are interrelated and the proper analysis of flexible conduits is complex. However, in order to develop a practically workable procedure, the designers of buried flexible conduits treat each failure condition separately.

In our paper an analytical approach to the study of the inelastic buckling of soil-steel structures is provided. This approach accounts for the large-strain formulation in the conduit walls through the geometric matrix [S]. However, it does not cover all

aspects such as the effect of soil failure or the inelastic soil behavior on the stability of the conduit. We invite other researchers to develop a non-linear coefficient of soil reaction that can reflect such conditions. These coefficients can be easily accommodated in the proposed analysis and will be an added step in the right direction.

The modulus of soil reaction,  $E_s = 8,000$  psi, applied in the examples for comparison with the OHBDC is based on the OHBDC recommendation.

## REFERENCES

1. Ontario Highway Bridge Design Code. Ministry of Transportation and Communications, Downsview, Ontario, Canada, 1984.
2. Standard Specifications for Highway Bridges, 11th ed. AASHTO, Washington, D.C., 1973.
3. R.K. Watkins and A.P. Moser. The Structural Performance of Buried Corrugated Steel Pipes. Research Report. Engineering Experiment Station, Utah State University, Logan, 1966.
4. M.G. Spangler. Underground Conduits--An Appraisal of Modern Research. Trans. ASCE, Vol. 113, 1948, pp. 316-341.
5. G.G. Meyerhof and L.D. Baika. Strength of Steel Culvert Sheets Bearing Against Compacted Sand Backfill. In Highway Research Record 30, HRB, National Research Council, Washington, D.C., 1963, pp. 1-19.
6. H.A. White and J.P. Layer. The Corrugated Metal Conduit as a Compression Ring. HRB Proc., Vol. 39, 1960, pp. 389-397.
7. M.G. Katona and J.M. Smith. CANDE: User's Manual. Naval Civil Engineering Laboratory, Port Hueneme, Calif., 1976.
8. K. Kloeppel and D. Glock. Theoretische und experimentelle untersuchungen zu den traglastproblemen biegeeweicher. Publication 10. Institut fuer Statik und Stahlbau, Darmstadt, Federal Republic of Germany, 1970.
9. J.M. Duncan. Behavior and Design of Long-Span Metal Culvert Structures. Presented at the Technical Session on Soil-Structure Interaction for Shallow Foundations and Buried Structures, ASCE, San Francisco, Calif., Oct. 1977.
10. J.A. Cheney. Buckling of Soil-Surrounded Tubes. Journal of the Engineering Mechanics Division, ASCE, Vol. 97, No. EM4, 1964, pp. 333-343.
11. G.A. Abdel-Sayed. Stability of Flexible Conduits Embedded in Soil. Canadian Journal of Civil Engineering, Vol. 5, 1978.
12. G.A. Leonards and R.E. Stetkar. Performance of Flexible Conduits. Interim Report. FHWA, U.S. Department of Transportation, 1978.
13. B.N. Okeagu. Analysis and Stability of Large-Span Flexible Conduits. Ph.D. thesis. Michigan State University, East Lansing, 1982.
14. B.N. Okeagu and G. Abdel-Sayed. Coefficients of Soil Reaction for Buried Flexible Conduits. Journal of Geotechnical Engineering, ASCE, July 1984.
15. C. Vijakhana and F. Nishino. Inelastic Stability of Unbraced Building Frames. Journal of the Structural Division, ASCE, March 1974.

Publication of this paper sponsored by Committee on Subsurface Soil-Structure Interaction.